

## USING THE WORLD'S LARGEST STRESS INTENSITY FACTOR DATABASE FOR FATIGUE LIFE PREDICTIONS

**Scott A. Fawaz**

Center for Aircraft Structural Life Extension (CAStLE)  
Department of Engineering Mechanics, United States Air Force Academy  
2354 Fairchild Drive, Ste 6L-155, USAF Academy, CO 80840, USA  
e-mail: [scott.fawaz@usafa.af.mil](mailto:scott.fawaz@usafa.af.mil)  
Web page: [www.usafa.af.mil/df/dfem/castle/](http://www.usafa.af.mil/df/dfem/castle/)

**Abstract.** *Population of the world's largest database of stress intensity factor ( $K$ ) solutions began in 2002 with the calculation of 5.6 million  $K$  solutions for diametrically opposed unsymmetric corner cracks at a straight shank hole in a finite width sheet subject to remote tension, remote bending, and bearing loading. For the last 20 years, the well-known Newman/Raju  $K$  solutions have been used for predicting fatigue life for the case of two cracks of the same shape and size. Differences between the Newman/Raju solutions and new  $K$ 's exist and the effect on inspection intervals and fatigue lives is assessed. In addition, the accuracy of engineering assumptions required to use the Newman/Raju solutions are evaluated. Overall, the correlation between the two solution sets was quite poor.*

### 1. INTRODUCTION

In assembling complex structures like military or commercial aircraft, riveted or bolted joints are primarily used as they offer many options to the designer. To satisfy fatigue requirements, the designer can either keep the stress levels below the endurance limit or ensure the slow crack growth life of the component is greater than the design service goal plus some factor of safety. The latter approach is most commonly used and relies on the ability to predict fatigue crack growth at fatigue critical locations. Fractographic information obtained from teardown and failure analysis of retired aircraft indicates that predicting growth of two unsymmetric (different crack length and/or crack depth) corner cracks on opposite sides of a fastener hole is necessary.<sup>1,2</sup> In a fracture mechanics context, the stress intensity factor,  $K$ , is required for such predictions. The seminal work in this area was completed by Newman and Raju.<sup>3</sup>

### 2. BACKGROUND

Several researchers have investigated the accuracy of the Newman/Raju (N/R)  $K$  equations<sup>4</sup>, which were derived from finite element analysis (FEA), for corner crack(s) growing from an open hole. Forman and Mettu conducted fatigue experiments of a single crack growing from a centrally located hole in titanium Ti-6AL-4V plates loaded by remote tension and remote bending (separately) and found good agreement between the experimental and predicted results; however, two additional fitting parameters had to be derived.<sup>5</sup> Fawaz, Andersson, and Newman fatigue tested two cracks growing from a centrally located hole in aluminum 7075-T651 and found poor correlation for the limited number of tests conducted.<sup>6</sup> Currently, a more extensive validation effort is underway in the CAStLE laboratory with the results to be reported in late 2007. An interesting observation in reference [6] and previously

in references [7] and [8] was that two corner cracks at a hole rarely propagate in equal increments and therefore are only symmetric at the beginning of the fatigue test. In a purely analytical investigation, Bakuckas compared the N/R solutions to those obtained from the equivalent domain integral method, semi-empirical equations, finite element alternating method, boundary element method, crack opening displacement method, and weight function method and found agreement within  $\pm 3\%$ . Fawaz and Andersson, using the *hp*-version finite element method (FEM), found similar agreement for a very limited set of crack length to crack depth ( $a/c$ ), crack depth to sheet thickness ( $a/t$ ), and hole radius to sheet thickness ( $r/t$ ) subject to remote tension. However, the  $K$  correlation was not as good for the following cases: bending loading, bearing loading, large  $a/t$  ( $> 0.8$ ),  $K$  at the crack depth,  $a$ , location, and  $K$  close to the intersection of the crack front and free surface.<sup>9</sup> With the difference in N/R and Fawaz/Andersson (F/A)  $K$  solutions well documented, the affect on inspection intervals and fatigue lives is investigated here.

### 3. ANALYTICAL INVESTIGATION

The fatigue life ( $N_f$ ), continuing damage analysis, initial inspection, and recurring inspection interval are the metrics used to assess the significance of the differences between the N/R and F/A  $K$  solutions. The global geometry is depicted in Figure 1. The geometric parameters are chosen to represent two different aircraft design challenges; a transport aircraft fuselage lap splice joint (thin skin) and a lower wing skin (thick skin). Of course, the analysis parameter space is in terms of non-dimensional quantities,  $a_1/c_1$ ,  $a_2/c_2$ ,  $a_i/t$ , and  $r/t$  thus the results are generally applicable. For the lap joint, the geometric quantities in millimeters are  $W = 29$ ,  $t = 1.6$ ,  $r = 2.4$  and for the wing skin  $W = 115$ ,  $t = 6.35$ ,  $r = 9.5$ . Four different load spectra are used constant amplitude (CA), Fighter Aircraft Loading STandard For Fatigue evaluation (FALSTAFF), Transport WIng STandard (TWIST), and marker. The CA spectrum was chosen to represent transport aircraft fuselage hoop stress. FALSTAFF and TWIST are standardized spectra commonly used to assess the performance of prediction models. The marker spectrum is often used in laboratory experiments to create marker bands on the fracture surface. To assess the sensitivity of the life predictions to applied loading, both remote tension and bending are applied simultaneously. The tension stress ratio ( $TSR$ ) is the remote tension stress normalized by a reference stress and similarly, the bending stress ratio ( $BSR$ ) is the remote bending stress normalized by a reference stress. Typically, the reference stress is the remote tension stress and this convention is adopted here. For all analyses,  $TSR = 1.0$  and  $BSR = 0.4$ . Two different maximum spectra stress, 69 and 124 MPa, were used to determine the sensitivity of the predictions to stress level. The stress levels used here represent the upper and lower bounds of transport aircraft fuselage hoop stress. To avoid variability in models that predict load sequence effects, neither crack retardation nor crack closure models were used. All analyses use 2024-T3 material and mechanical properties available in AFGROW.<sup>10</sup>

The results of the fatigue life predictions comparing the N/R and F/A  $K$  solutions are in the form,  $e_0 = (N_{f_{N/R}} - N_{f_{F/A}}) / N_{f_{F/A}}$ . Fatigue lives of large cracks,  $a_1 = c_1 = a_2 = c_2 = 1.27$  mm, and small cracks,  $a_1 = c_1 = a_2 = c_2 = 0.32$  mm for a thin skin are shown in Figure 2 and

Figure 3; respectively. The former is the required damage tolerance flaw size as prescribed by JSSG 2006<sup>11</sup> and the latter is used in durability analyses. Figure 4 shows the results of a damage tolerant flaw in a thick skin. In addition, both the single corner crack at a hole and symmetric corner cracks at a hole are analyzed.

In the USAF fleet, the aircraft structural integrity engineers follow the initial flaw assumption and continuing damage requirements as outlined in reference [11]. To give context to the differences in the life predictions obtained from the N/R and F/A  $K$  solutions, the geometry considered here, in JSSG 2006 terms, is one of the following; slow crack growth, fail-safe primary element, or fail-safe adjacent structure. With these assumptions, the initial flaw size,  $a_i$ , is 1.27 mm and the continuing damage size  $0.127 \text{ mm} + \Delta a$ . The initial flaw size is rather straight forward; however, how to determine  $\Delta a$  requires some explanation. To calculate  $\Delta a$ , phase I of the analysis is to propagate a single corner crack from  $a_i$  to failure. What constitutes “failure” is determined by the analyst but is most commonly the crack growing to the next fastener hole or part edge, also known as the remaining ligament. This approach is not used here since in doing so additional  $K$  solutions are required which could make assessing the difference between the N/R and F/A solutions more difficult. For all analyses here, failure is defined as a corner crack growing through 99% of the sheet thickness ( $a/t = 99\%$ ). Since the F/A  $K$  solutions include very deep cracks,  $a/t = 95\%$ , letting the analysis proceed to  $a/t = 99\%$  will ensure the  $a/t = 95\%$  results are used. With the phase I analysis complete, the number of cycles,  $N_{\text{phase I}}$ , from  $a_i$  to failure is known. Phase II of the analysis is to determine  $\Delta a$ . Similarly, a single corner crack of 0.127 mm (known as the continuing damage flaw size,  $a_{cd}$ ; note  $a_{cd} \neq a_i$ ) is propagated only to the number of cycles determined in phase I,  $N_{\text{phase I}}$ . The resulting crack length at  $N_{\text{phase I}}$  is  $\Delta a$ . The continuing damage methodology outlined above was developed since  $K$  solutions for unsymmetric corner cracks at a hole have not been available in any life prediction code until 2005.<sup>11</sup> Now that these new solutions are available, the continuing damage scenario can be analyzed explicitly.

For the continuing damage scenario as outlined above, the results of predictions using the N/R and F/A  $K$  solutions is assessed in two parts. Part one,  $N_{\text{phase I}}$  is calculated using the N/R solutions, phase I above, and is compared to the number of cycles,  $N_1$ , using the F/A  $K$  solutions to propagate  $a_1 = c_1 = 1.27 \text{ mm}$  ( $a_2 = c_2 = 0.127 \text{ mm}$ ) to failure. The metric  $e_1 = (N_{\text{phase I}} - N_1)/N_1$  is used. The results of the phase I fatigue life comparisons are shown in Figure 5 and Figure 6. Part two, the  $\Delta a$  for the N/R and F/A solutions are compared in Figure 7 and Figure 8 using the metric  $e_2 = (\Delta a_{\text{N/R}} - \Delta a_{\text{F/A}})/\Delta a_{\text{F/A}}$ . For simplicity,  $\Delta a$  is used generically and represents the growth of the continuing damage crack,  $a_{cd}$ , for both the crack length,  $c$ , and crack depth,  $a$ , directions.

The last method used to assess the predictions using the N/R and F/A  $K$  solutions is the affect on the initial ( $I$ ) and recurring ( $H$ ) inspection intervals. These two inspection intervals can be easily calculated using  $I = (N_{a_{\text{critical}}} - N_{a_{\text{ASIP}}})/2$  and  $H = (N_{a_{\text{critical}}} - N_{a_{\text{NDI}}})/2$ . Where  $N_{a_{\text{critical}}}$  is the number of cycles to reach the critical crack size,  $N_{a_{\text{ASIP}}}$  is the number of cycles to reach the initial flaw size ( $a_{\text{ASIP}}$ ), and  $N_{a_{\text{NDI}}}$  is the number of cycles when the crack can be detected by non-destructive inspection (NDI) techniques. In all analyses conducted in this effort,  $N_{a_{\text{ASIP}}} = 0$ ; thus  $I = N_{a_{\text{critical}}}/2$ ; thus, Figure 2 - Figure 4 can be used to assess

the effect on  $I$ . A common inspection technique for fastener holes is bolt hole eddy current (BHEC) which requires the removal of the fastener. The detectable crack size for BHEC is 1.27 mm ( $a_{NDI}$ ) with 90% probability of finding the crack with 95% confidence.<sup>12</sup> Since  $a_{ASIP} = a_{NDI} = 1.27$  mm and  $N_{a_{ASIP}} = N_{a_{NDI}} = 0$ , the initial inspection and recurring inspection interval are equal,  $I = H = N_{a_{critical}}/2$ .

#### 4. DISCUSSION

The results of all the analyses are discussed in the three sections below. Each of the metrics is in terms of  $e_0$ ,  $e_1$ , and  $e_2$  which are relative percent differences between the results produced by the N/R and F/A  $K$  solutions as defined in section 3.

##### 4.1. FATIGUE LIFE

The assessment of the fatigue lives is determined from the data presented in Figure 2 - Figure 4. For the thin skin small single crack case in Figure 2, the N/R solutions on average yield a fatigue life 39% longer than the F/A solutions. The difference is much larger for the thin skin large single crack case, Figure 3, where the N/R results are 174% larger than the F/A results. The thick skin single damage tolerant flaw, Figure 4, the difference is 42% which is quite similar to the results in Figure 2. The trends are the same for the double crack case, again in Figure 2 - Figure 4, where the N/R results are larger by 27%, 130%, 29%; respectively. For the double crack case, the differences are attributed to the known difference in the  $K$  solutions.<sup>6,9</sup> The N/R solutions were developed for  $0.2 \leq a/t \leq 0.8$ . For the small crack results where  $a/t$  starts at 0.2, the small difference in the two sets of  $K$  solutions for remote tension loading is evident. However, for the large crack results,  $a/t \geq 0.8$ , the extrapolation error for the N/R solutions is quite large. For both the small and large cracks, the single crack results show larger differences between the two sets of solutions. In addition to the source of the difference for the double crack case, the single crack case also shows the error in using the Shah correction factor.<sup>13</sup> Shah developed a correction factor to convert  $K$  solutions derived for two symmetric cracks to a  $K$  solution for a single crack. Errors in the Shah correction factor were also reported in reference [9]. In comparing Figure 2 and Figure 4, the non-dimensional crack geometry is the same but the difference is slightly larger for the latter which is due to the overall higher fatigue life and the corresponding error that accumulates over the larger number of cycles.

For the small cracks, no systemic trends amongst the various fatigue spectra and maximum stress levels are apparent. However, for the single and double large cracks, the difference in solutions is largest for the CA and marker spectra at the low maximum stress level. A possible reason for this behavior is that at the low maximum stress level, the crack growth is slow and more cycles are applied to the crack where the difference in the  $K$  solutions is largest.

##### 4.2. CONTINUING DAMAGE SCENARIO

The continuing damage scenario is assessed using the results in Figure 5 - Figure 8. In

Figure 5 and Figure 6, the number of fatigue cycles in phase I is compared. Again, the differences in the fatigue life results, 42% and 219% on average for the thin and thick skin; respectively, is attributed to two phenomena; one, the inherent differences in  $K$ 's calculated using the  $hp$ -version FEM (F/A solutions) and the  $h$ -version FEM (N/R with one order of magnitude less degrees of freedom in the FEM); two, the shortcomings of the continuing damage scenario methodology as outlined in section 3. The differences are largest at the lowest CA and marker spectra maximum stress levels for the same reason discussed in section 4.1. For the standard fatigue spectra, FASTAFF and TWIST, no significant differences are evident. A special beta version of the crack growth code AFGROW<sup>10</sup> was used for all predictions and a trivial bug, which was fixed after this paper was submitted, was discovered which affected the standard stress spectra analyses in Figure 6 - Figure 8. Thus, if a particular result is omitted, it was affected by the bug.

In Figure 7 and Figure 8, the effect on the phase II crack length,  $\Delta a$ , is evaluated. Except for the low maximum stress level of the FALSTAFF analysis, the N/R  $K$  solutions predict a longer crack length than that predicted by the F/A  $K$  solutions. This result is not unexpected in view of the data in Figure 5 and Figure 6. Cracks propagated with the N/R  $K$  solutions grow longer in phase I; therefore their size must also be larger in phase II.

### 4.3. INSPECTION INTERVALS

The initial inspection and the recurring inspection interval are the same,  $I = H = N_{a_{critical}}/2$ . For all the cracking scenarios, spectra, and maximum stress levels results presented in Figure 2 - Figure 4, the N/R  $K$  solutions produce non-conservative initial inspections and recurring inspection intervals as compared to the F/A solutions. In other words, the initial inspection is not occurring early enough in the aircraft life and the recurring inspections are not occurring as often as required. These results are consistent with the  $K$  solution validation reported in reference [6].

## 5. CONCLUSION

In this analytical investigation, fatigue life predictions were made using the Newman/Raju and Fawaz/Andersson stress intensity factor solutions as implemented in the USAF life prediction code, AFGROW. The differences were assessed in terms of fatigue life and crack length. For the fatigue life predictions, differences (20 - 270%) were found for all scenarios considered with the most significant differences for the thin skin geometry. Shortcomings in the Shah correction factor (8 - 50%) and the JSSG 2006 continuing damage scenario (38 - 350%) were also discovered. For the crack length predictions in the continuing damage scenario, the low stress level FALSTAFF results showed perfect correlation; whereas the other spectra and stress levels showed differences as large as 47%. The underlying cause of the differences is that the Newman/Raju solutions in general under-predict  $K$  which confirms the conclusions presented in reference [6] and [9]. Furthermore, under-predicting  $K$  leads to over-predicting fatigue life which is non-conservative in terms of flight safety. With the new Fawaz/Andersson solutions now available, more accurate fatigue life predictions of unsymmetric corner cracks at a hole subject to tension, bending and bearing loading are

possible.

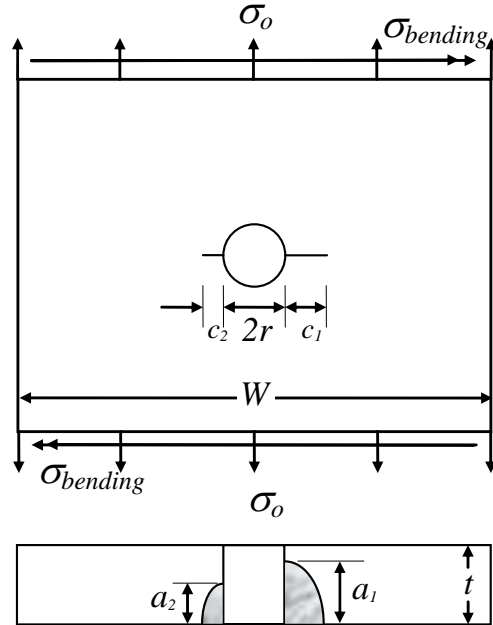


**Figure 1** Global geometry used for all analyses

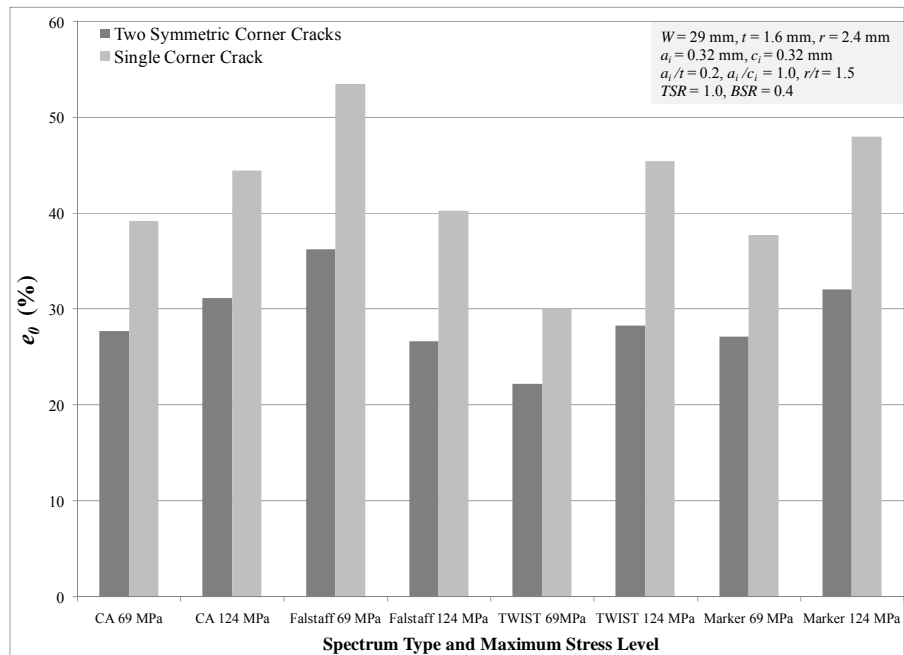


**Figure 2** Comparison of small crack analyses in a thin skin for single/double corner cracks, four fatigue spectra, and two maximum stress levels

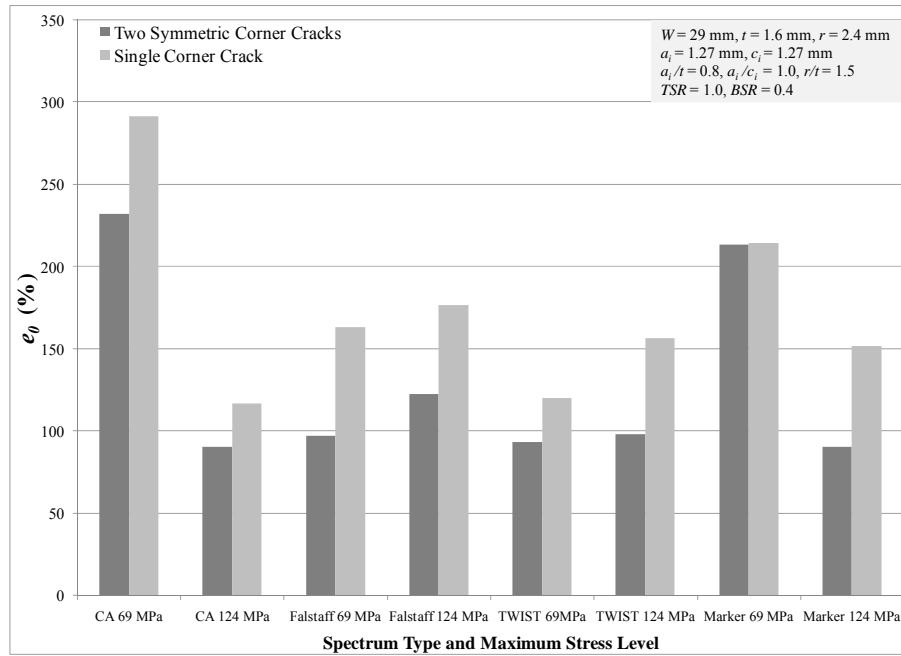


**Figure 3 Comparison of large crack analyses in a thin skin for single/double corner cracks, four fatigue spectra, and two maximum stress levels**

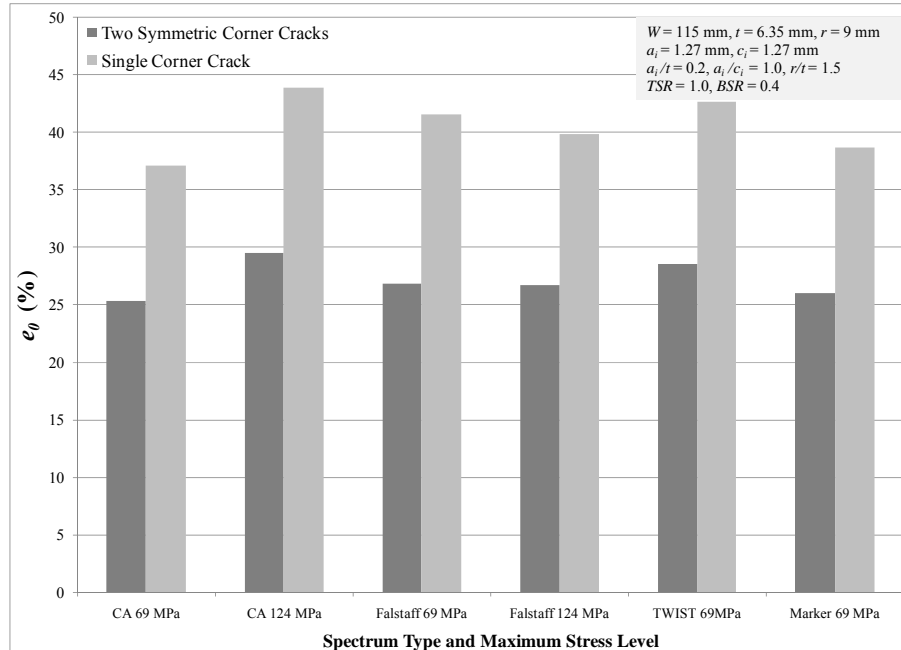


**Figure 4 Comparison of a damage tolerant flaw analyses in a thick skin for single/double corner cracks, four fatigue spectra, and two maximum stress levels**

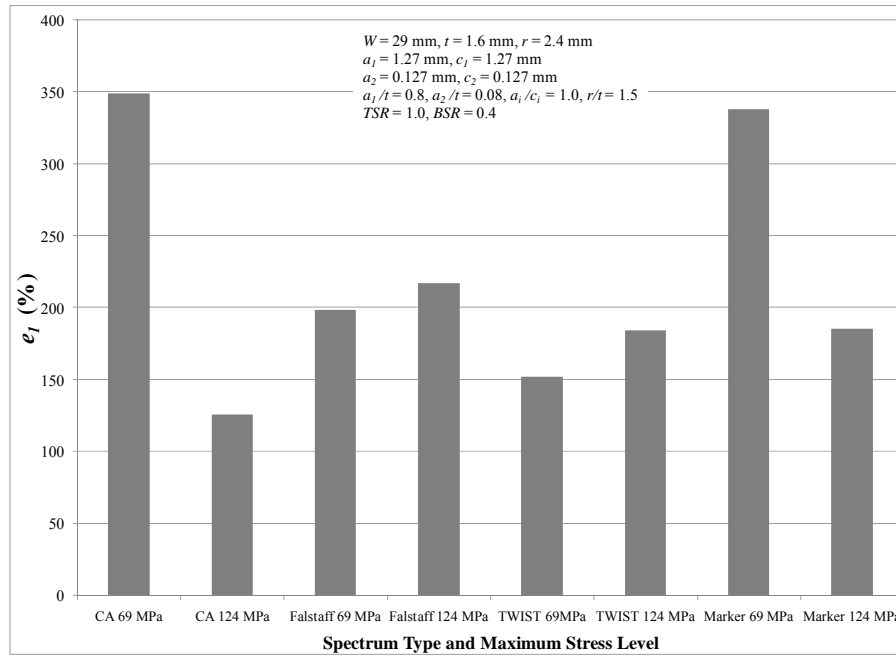


Figure 5 Comparison of continuing damage scenario analyses for a damage tolerant flaw in a thin skin

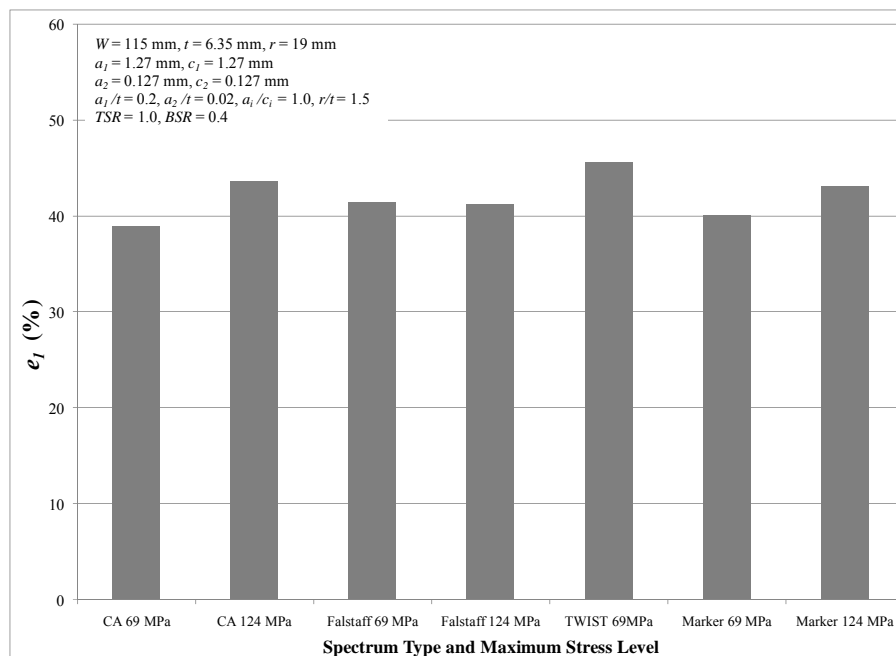


Figure 6 Comparison of continuing damage scenario analyses for a damage tolerant flaw in a thick skin

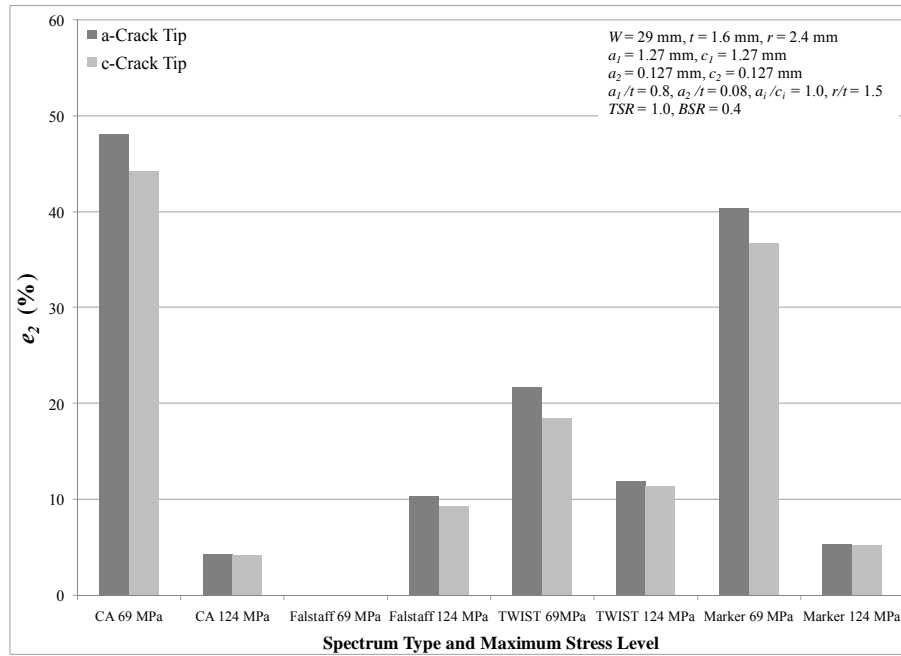


Figure 7 Comparison of  $\Delta a$  for the continuing damage scenario analyses in a thin skin

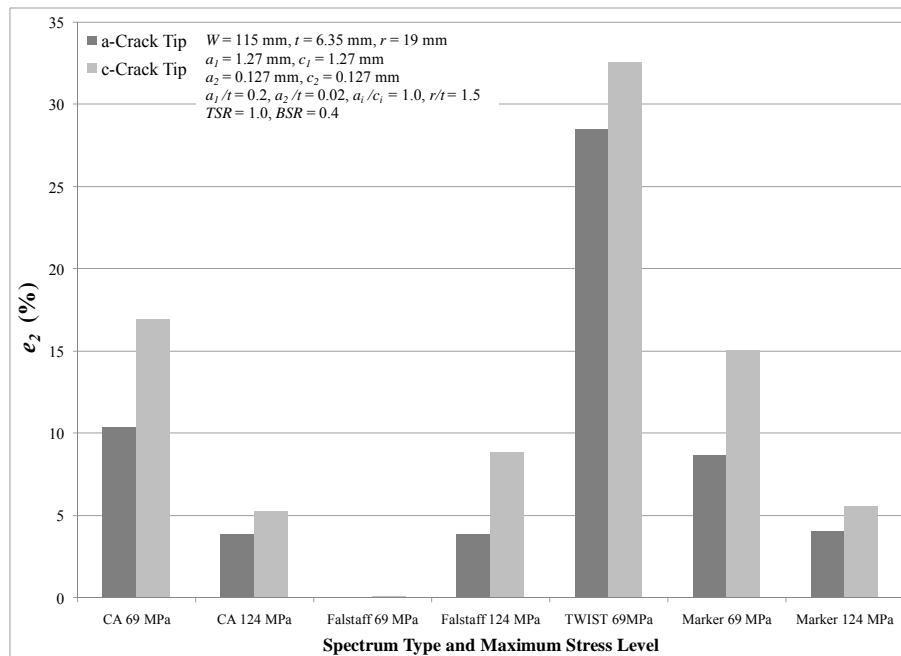


Figure 8 Comparison of  $\Delta a$  for the continuing damage scenario analyses in a thick skin

- [1] Piascik, Robert S., Scott A. Willard, and Matthew Miller. *The Characterization of WideSpread Fatigue Damage in Fuselage Structure*. NASA-TM-109142, 1994.
- [2] Shoales, G. and P. Christiansen, C-130 Center Wing Box Structural Teardown Analysis Program, Proc. at the 24<sup>th</sup> International Committee on Aeronautical Fatigue Symposium, Naples, Italy, 16 - 18 May 2007.
- [3] Raju, I. S. and J. C. Newman, Jr., Stress Intensity Factors for Two Symmetric Corner Cracks, *Fracture Mechanics*, ASTM STP 677, American Society for Testing and Materials, Ed. C. W. Smith, 1979, pp. 411-430.
- [4] Newman, Jr., J. C. and I. S. Raju. *Stress Intensity Factor Equations for Cracks in Three-Dimensional Finite Bodies Subjected to Tension and Bending Loads*. NASA-TP-85793, 1984.
- [5] Forman, R. G., and S. R. Mettu. Behavior of Surface and Corner Cracks Subjected to Tensile and Bending Loads in Ti-6Al-4V Alloy. *Fracture Mechanics: Twenty-Second Symposium*, Vol. 1, ASTM STP 1131, H. A. Ernst, A. Saxena, and D. L. McDowell, Eds., American Society for Testing and Materials, Philadelphia, 1992. 519-546.
- [6] Fawaz, S. A., Börje Andersson and J. C. Newman, Jr. Experimental Verification of Stress Intensity Factor Solutions for Corner Cracks at a Hole Subject to General Loading. Proc. of the 22<sup>nd</sup> Symposium of the International Committee on Aeronautical Fatigue, 7-9 May 2003, Lucerne, CH, EMAS.
- [7] Fawaz, S. A. and J. Schijve. Multiple Site Damage in a Pressurized Fuselage Riveted Lap Joint. Proc. of the 1994 USAF Structural Integrity Program Conference, 6-8 Dec 1994, San Antonio, TX, WL-TR-96-4030.
- [8] Fawaz, S. A. A Thin-Sheet, Combined Tension and Bending Specimen. *International Journal of the Society of Experimental Mechanics*. Vol. 39.3 (1999): 171-176.
- [9] Fawaz, S. A. and Börje Andersson. Accurate Stress Intensity Factor Solutions for Unsymmetric Corner Cracks at a Hole. Proc. of the Fourth Joint DoD/FAA/NASA Conference on Aging Aircraft, 15-18 May 2000, St. Louis, MO.
- [10] Harter, James A., "AFGROW Users Guide and Technical Manual, AFGROW version 4.0012.15," AFRL-VA-WP-TR-2007, February 2007.
- [11] *Joint Service Specification Guide on Aircraft Structures*, JSSG-2006, 30 October 1998.
- [12] Brausch, John, C., Personal Communication, The Air Force Research Laboratory, Materials Directorate, Systems Support Division, 19 July 2007.
- [13] Shah, R. C., Stress Intensity Factors for Through and Part Through Cracks Originating at Fastener Holes, *Mechanics of Crack Growth*, ASTM STP 590, American Society for Testing and Materials, 1976, pp. 429-459.